



# The use of the structural correlation method for the estimation of the quality of ab initio and DFT predictions of geometry parameters of related compounds in the gas phase and in solutions. An example of (O–Si)chelates with ClSiC<sub>3</sub>O coordination center

E.F. Belogolova<sup>a</sup>, E.P. Doronina<sup>a</sup>, M.A. Belogolov<sup>b</sup>, V.F. Sidorkin<sup>a,\*</sup>

<sup>a</sup>A.E. Favorsky Irkutsk Institute of Chemistry, Siberian Branch of the Russian Academy of Sciences, Favorsky 1, Irkutsk 664033, Russia

<sup>b</sup>East Siberian Institute of Russian Ministry for Internal Affairs, Lermontov 110, Irkutsk 664077, Russia

## ARTICLE INFO

### Article history:

Received 6 February 2010

Accepted 24 March 2010

Available online 29 March 2010

### Keywords:

Pentacoordinated silicon compounds

Structural correlation

Bond order

Reaction path

Quantum chemical calculation

## ABSTRACT

X-ray data on the intramolecular complexes **1–4** (*N*-dimethylchlorosilylmethyl derivatives of amides, lactams, carbamides, and hydrazides of carbon acids) possessing an identical ClSiC<sub>3</sub>O coordination center have been used for mapping the path of the S<sub>N</sub>2 substitution reaction at Si<sup>IV</sup> with the Bürgi–Dunitz method. A classic hyperbolic like representation of the reaction coordinate has been obtained using the nonlinear least squares method. The hypothesis of the unified character of the change in geometry parameters of the ClSiC<sub>3</sub>O reaction center in **1–4** under the influence of internal factors and the medium is corroborated based on the study of ab initio and DFT gas-phase and solution structures of a series **1–4**. The extent of deviation of calculated points from the correlation function, defined by the collective body of X-ray data for the coordination center of related compounds, may be used as an indicator of the accuracy of their geometry calculation in the isolated state and, especially, in solutions.

© 2010 Elsevier B.V. All rights reserved.

## 1. Introduction

A “static” approach (the structural correlation method, SCM) proposed by Bürgi and Dunitz [1–3] has been widely used to solve the diversified problems of the chemical dynamics [1–11]. In the framework of SCM the modeling of chemical transformations is performed by a set of equilibrium crystal structures of complexes containing the fragment of interest (coordination center hereinafter CC), identical with the reaction center. The gradual distortion or static deformation that the molecular fragment manifests collectively over a large variety of crystalline frameworks mirrors the distortion which that fragment would undergo along a given reaction coordinate. Figuratively speaking, each structure from the set is considered as a ‘frozen-in’ point taken along the studied reaction pathway (RP).

In the framework of the Bürgi–Dunitz method, the relationship of structure correlations to reaction profiles is expressed in the structure correlation hypothesis. This hypothesis suggests that if a correlation can be found between two or more independent parameters describing the structure of a given structural fragment in a variety of environments, then the correlation function (CF)

maps a minimum energy path in the corresponding parameter space [12].

The laws governing chemical bonding and intermolecular interactions are essentially the same in the gas phase, in solid, and in solutions [3]. Thus, the search of CF for a coordination center may be in principle performed using the structural parameters of related compounds determined in any their phase state. Because of the scant information on the geometry of inter- and intramolecular complexes for the gas phase and its total absence for solution, the corroboration of this conclusion has not been yet obtained.<sup>1</sup> However, necessary information on the structure of molecules in their isolated states and in solutions may be provided also by quantum chemistry methods. Thus, it is reasonable to propose that the large-magnitude root-mean square deviations ( $\chi^2$ ) of theoretical points from the high quality CF, found using X-ray data, may be a consequence of the approximate character of calculation methods and solvation models. It is tempting to use this circumstance for the original evaluation of the reliability of ab initio

<sup>1</sup> The reaction of complex formation of boranes with amines [13] may be cited as a rare example when for the modeling of RP it was possible to invoke not only the X-ray solid-state structures, but also the gas-phase (microwave spectroscopy) ones. It turns out that the structures go well together and make it possible to describe the reaction coordinate more precisely.

\* Corresponding author. Tel.: +7 3952 424871; fax: +7 3952 419346.  
E-mail address: [svf@irioch.irk.ru](mailto:svf@irioch.irk.ru) (V.F. Sidorkin).



H-complexes of (O–Si)chelates

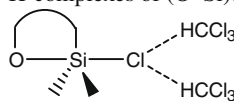


Chart 2.

An analytical representation of the reaction path of Eq. (1) was obtained applying the nonlinear least squares method [37]. The applied approach is based on minimization of the chi-squared ( $\chi^2$ ):

$$\chi^2 = (1/\nu) \sum_{i=1}^N [f(x_i) - y_i]^2, \quad (2)$$

where  $(x_i, y_i)$  are the coordinates of points corresponding to the structures **1–4**, therewith  $x = d_{\text{Si–O}}$ ,  $y = d_{\text{Cl–Si}}$ ;  $f(x_i)$  is the fitted function describing these points,  $\nu = N - n$  is the degrees of freedom,  $N$  is the number of points, and  $n$  is the number of coefficients of parameters used in the regression fit. For the estimation of the extent of deviation of ab initio and DFT calculated points from the function  $f(x)$  describing the reaction path we used the parameter  $\chi^2$  putting  $n = 0$ .

### 3. Results and discussion

#### 3.1. A modeling of the $S_N2$ type reaction at $\text{Si}^{\text{IV}}$ with the set of structures **1–4**

According to the main idea of SCM, a considerable interval of the change in the X-ray internuclear distances Cl–Si ( $d_{\text{Cl–Si}}$ ) and Si–O ( $d_{\text{Si–O}}$ ) in the series **1–4** (see Table 1) allows to reconstruct a significant part of the  $S_N2$  substitution reaction path at the silicon atom including the region of Walden inversion of its configuration (Eq. (1)) with this set of structures (intermediate complexes **B**).

For the reactions of this type (Eq. (1)) proceeding with the cleavage of one univalent bond and the formation of another one, the sum of bond orders of the axial Cl–Si and Si–O bonds ( $N_{\text{Cl–Si}}$  and  $N_{\text{Si–O}}$ ) in any point of RP (Eq. (1)) is constant by definition [45–47], and is equal to unity:

$$N_{\text{Cl–Si}} + N_{\text{Si–O}} = 1 \quad (3)$$

**Table 1**  
X-ray geometrical parameters (Å) of the  $\text{ClSiC}_3\text{O}$  coordination center for species **1–4**.

| Compound  | $d_{\text{Si–O}}^a$ | $d_{\text{Cl–Si}}^a$ | $\Delta_{\text{Si}}^b$ | Ref. |
|-----------|---------------------|----------------------|------------------------|------|
| <b>1a</b> | 2.450               | 2.154                | 0.322                  | [38] |
| <b>1b</b> | 1.954               | 2.307                | 0.058                  | [23] |
| <b>1c</b> | 1.950               | 2.315                | 0.055                  | [23] |
| <b>1d</b> | 1.939               | 2.321                | 0.055                  | [39] |
| <b>1e</b> | 2.021               | 2.282                | 0.082                  | [23] |
| <b>1f</b> | 2.050               | 2.284                | 0.099                  | [23] |
| <b>1g</b> | 1.989               | 2.307                | 0.060                  | [38] |
| <b>1g</b> | 1.988               | 2.312                | 0.074                  | [38] |
| <b>1h</b> | 2.171               | 2.210                | 0.190                  | [40] |
| <b>1i</b> | 2.050               | 2.271                | 0.110                  | [41] |
| <b>2a</b> | 2.077               | 2.229                | 0.134                  | [42] |
| <b>2a</b> | 2.027               | 2.259                | 0.160                  | [42] |
| <b>2b</b> | 1.918               | 2.348                | 0.027                  | [23] |
| <b>2c</b> | 1.974               | 2.307                | 0.050                  | [43] |
| <b>2d</b> | 1.975               | 2.294                | 0.077                  | [23] |
| <b>2e</b> | 1.923               | 2.316                | –                      | [44] |
| <b>2f</b> | 2.142               | 2.223                | 0.187                  | [23] |
| <b>3a</b> | 1.879               | 2.432                | –0.078                 | [23] |
| <b>3c</b> | 1.788               | 2.624                | –0.178                 | [23] |
| <b>4</b>  | 1.840               | 2.438                | –0.073                 | [25] |

<sup>a</sup>  $d_{\text{Si–O}}$  and  $d_{\text{Cl–Si}}$  are the Si–O and Cl–Si bond distances.

<sup>b</sup>  $\Delta_{\text{Si}}$  is the displacement of the silicon atom out of the plane of three carbon atoms.

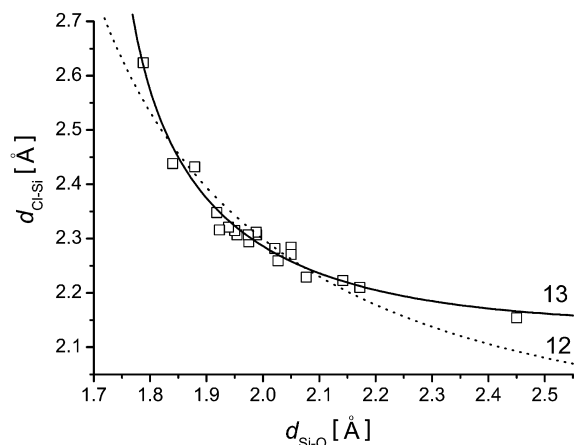


**Fig. 1.** Relationship between the X-ray internuclear Si–O and Cl–Si distances ( $d$ , Å) in compounds **1–4** and the position of the experimental points relative to the curves defined by Eqs. (12) and (13).

The bond orders  $N_{\text{Cl–Si}}$  and  $N_{\text{Si–O}}$  can be obtained from the corresponding bond lengths ( $d_{\text{Cl–Si}}$  and  $d_{\text{Si–O}}$ ) using the Pauling relationship [48]:

$$\Delta d_i = C \log N_i \quad (4)$$

where  $\Delta d_i = d_i - d_i^0$  ( $i = \text{Cl–Si, Si–O}$ ) is the change in the internuclear distances Cl–Si and Si–O for complexes **B** with respect to the lengths of  $d_{\text{Cl–Si}}^0$  and  $d_{\text{Si–O}}^0$  covalent bonds with  $N = 1$  corresponding to the noncholate form **A** (reagent) and to the cation **C** (product), respectively;  $C$  is a constant which can be different for the Cl–Si and Si–O contacts ( $C_1$  and  $C_2$ ).

In view of Eq. (4), Eq. (3) represents the hyperbolic like function:

$$10^{-(\Delta d_{\text{Cl–Si}}/C_1)} + 10^{-(\Delta d_{\text{Si–O}}/C_2)} = 1. \quad (5)$$

The relationship between the  $d_{\text{Cl–Si}}$  and  $d_{\text{Si–O}}$  values (see Table 1) in a series of structures **1–4**, presented in Fig. 1, is really of the hyperbolic like type being characteristic for  $S_N2$  reactions [3,8,45].

Parameters of this function (Eq. (5)) are usually found using the definition<sup>2</sup> [49] of the bond orders of the Cl–Si and Si–O bonds in complexes **1–4** in terms of geometry parameters of their  $\text{ClSiC}_3\text{O}$  silicon polyhedron [24,25]:

$$\begin{cases} N_{\text{Cl–Si}} = (\Delta_{\text{Si}}^{\text{max}} + \Delta_{\text{Si}}) / 2\Delta_{\text{Si}}^{\text{max}} \\ N_{\text{Si–O}} = (\Delta_{\text{Si}}^{\text{max}} - \Delta_{\text{Si}}) / 2\Delta_{\text{Si}}^{\text{max}} \end{cases} \quad (6)$$

where  $\Delta_{\text{Si}}$  is the displacement of the silicon atom out of the plane of three carbon atoms in **1–4**, and  $\Delta_{\text{Si}}^{\text{max}}$  is the same in the reagent **A** (product **C**).

Eq. (4) can be written, in view of Eq. (6), in two forms (Eqs. (7) and (8)).

$$\begin{cases} \Delta d_{\text{Cl–Si}} = C_1 \log((\Delta_{\text{Si}}^{\text{max}} + \Delta_{\text{Si}}) / 2\Delta_{\text{Si}}^{\text{max}}) \\ \Delta d_{\text{Si–O}} = C_2 \log((\Delta_{\text{Si}}^{\text{max}} - \Delta_{\text{Si}}) / 2\Delta_{\text{Si}}^{\text{max}}) \end{cases} \quad (7)$$

$$\Delta d_{\text{Cl–Si, Si–O}} = C \log((\Delta_{\text{Si}}^{\text{max}} \pm \Delta_{\text{Si}}) / 2\Delta_{\text{Si}}^{\text{max}}), \quad (8)$$

where the plus sign refers to the Cl–Si bond and the minus sign refers to the Si–O bond.

<sup>2</sup> Eq. (6) is not the only representation of the Cl–Si and Si–O bond orders of complexes **1–4** in terms of geometrical characteristics of their silicon  $\text{ClSiC}_3\text{O}$  polyhedron. To a lesser extent the equations  $[N_{\text{Cl–Si}} = (1 - 3\cos\varphi)/2, N_{\text{Si–O}} = (1 + 3\cos\varphi)/2]$ , where  $\varphi$  is the mean Cl–Si–C bond angle between an axial bond and equatorial ones in the  $\text{ClSiC}_3\text{O}$  fragment] are used.

**Table 2**MP2 and DFT selected gas-phase bond distances ( $d$  [Å]) and root mean square deviations  $\chi^2$  from the hyperbole of Eq. (13) for species **1a–b**, **2a**, and **3a–b**.

| Method              | <b>1a</b>         |                    | <b>1b</b>         |                    | <b>2a</b>         |                    | <b>3a</b>         |                    | <b>3b</b>         |                    | $\chi^2$ |
|---------------------|-------------------|--------------------|-------------------|--------------------|-------------------|--------------------|-------------------|--------------------|-------------------|--------------------|----------|
|                     | $d_{\text{Si-O}}$ | $d_{\text{Si-Cl}}$ | $d_{\text{Si-O}}$ | $d_{\text{Si-Cl}}$ | $d_{\text{Si-O}}$ | $d_{\text{Si-Cl}}$ | $d_{\text{Si-O}}$ | $d_{\text{Si-Cl}}$ | $d_{\text{Si-O}}$ | $d_{\text{Si-Cl}}$ |          |
| MP2/6-31G(d)        | 2.578             | 2.127              | 2.223             | 2.172              | 2.263             | 2.153              | 2.118             | 2.196              | 2.005             | 2.234              | 0.0013   |
| MP2/6-311++G(d,p)   | 2.682             | 2.117              | 2.330             | 2.155              | 2.334             | 2.143              | 2.206             | 2.178              | 2.027             | 2.235              | 0.0010   |
| BP86/6-31G(d)       | 2.500             | 2.176              | 2.221             | 2.219              | 2.251             | 2.200              | 2.125             | 2.245              | 2.014             | 2.290              | 0.0002   |
| B3LYP/6-31G(d)      | 2.629             | 2.155              | 2.248             | 2.207              | 2.282             | 2.187              | 2.123             | 2.240              | 1.996             | 2.292              | 0.0001   |
| B3PW91/6-31G(d)     | 2.509             | 2.155              | 2.195             | 2.202              | 2.233             | 2.181              | 2.091             | 2.230              | 1.985             | 2.274              | 0.0002   |
| B3PW91/6-311G(2d,p) | 2.532             | 2.153              | 2.212             | 2.203              | 2.251             | 2.181              | 2.100             | 2.234              | 1.966             | 2.291              | 0.0001   |
| M05-2X/6-31G(d)     | 2.546             | 2.163              | 2.127             | 2.234              | 2.170             | 2.212              | 2.046             | 2.259              | 1.958             | 2.304              | 0.0001   |

In the variant  $C_1 \neq C_2$ , an apparent nonequivalence of the Cl–Si and Si–O bonds is emphasized, and at  $C_1 = C_2 = C$ , a representation of the reaction coordinate from Eq. (3) in the ideal form of Eq. (5) is more justified [50].

Invoking the experimental X-ray values ( $d_{\text{Si-O}}^0(\text{exp}) = 1.639$  Å,  $d_{\text{Cl-Si}}^0(\text{exp}) = 2.065$  Å and  $\Delta_{\text{Si}}^{\text{max}}(\text{exp}) = 0.60$  Å), which are characteristic of the model compounds of the tetracoordinate silicon and recommended in Ref. [24], we have obtained an explicit form of the linear regression (Eqs. (7) and (8)):

$$\begin{cases} \Delta d_{\text{Cl-Si}} = -1.348 \log[1.180 \cdot (\Delta_{\text{Si}}^{\text{max}} + \Delta_{\text{Si}})/2\Delta_{\text{Si}}^{\text{max}}]; \\ R = 0.98, sd = 0.02 \\ \Delta d_{\text{Si-O}} = -1.448 \log[1.298 \cdot (\Delta_{\text{Si}}^{\text{max}} - \Delta_{\text{Si}})/2\Delta_{\text{Si}}^{\text{max}}]; \\ R = .97, sd = 0.03 \end{cases} \quad (9)$$

$$\Delta d_{\text{Cl-Si-Si-O}} = -1.313 \log[1.194 \cdot (\Delta_{\text{Si}}^{\text{max}} \pm \Delta_{\text{Si}})/2\Delta_{\text{Si}}^{\text{max}}]; \\ R = .97, sd = 0.03 \quad (10)$$

This allowed us to give expressions, which represent the coordinate of reaction (Eq. (1)) in terms of the sum of axial bond orders:

$$10^{-(\Delta d_{\text{Cl-Si}}/1.348)} + 10^{-(\Delta d_{\text{Si-O}}/1.448)} = 1.239 + f(\Delta_{\text{Si}}), \quad (11)$$

$$10^{-(\Delta d_{\text{Cl-Si}}/1.313)} + 10^{-(\Delta d_{\text{Si-O}}/1.313)} = 1.194 \quad (12)$$

In the case of Eq. (11) the interval of the change in the value of the function  $f(\Delta_{\text{Si}}) = -0.098 \Delta_{\text{Si}}$  is not greater than 0.03 in a series of complexes **1–4**. Thus, the total order of the axial Cl–Si and Si–O bonds is constant with a good precision in the series **1–4**, irrespective of the form of presentation of the linear correlation (Eqs. (7) or (8)). At the same time, for the hyperbolic like functions of Eqs. (11) and (12), similar to functions found previously [24,25], the  $N_{\text{Cl-Si}} + N_{\text{Si-O}}$  sum is significantly larger than unity in their equations and hence the natural initial and final conditions for the reaction of Eq. (1) (at  $N_{\text{Cl-Si}}(N_{\text{Si-O}}) \rightarrow 1$ ,  $N_{\text{Si-O}}(N_{\text{Cl-Si}}) \rightarrow 0$ ) are not satisfied.

A moderate quality of the reaction coordinates (Eqs. (11) and (12)) may arise from the expected differences between the  $d_{\text{Si-O}}^0$ ,  $d_{\text{Cl-Si}}^0$  and  $\Delta_{\text{Si}}^{\text{max}}$  values of the reactant **A** (product **C**) for the process of Eq. (1) and the values of the forcedly invoked model compounds [8]. It is not feasible to perform their correct experimental choice. However, an effort can be made to find the representation of the reaction path (Eq. (1)) in the ideal form (Eq. (5)) without using a specific definition of bond orders and experimental values of  $d_{\text{Si-O}}^0$ ,  $d_{\text{Cl-Si}}^0$  and  $\Delta_{\text{Si}}^{\text{max}}$ . Drawing on the nonlinear least squares method, we performed the search for the parameters  $C$  and  $d_i^0$  for the function of Eq. (5) in a way that it would give the best fit to a set of experimental points **1–4**. Three such optimal parameters were found:  $d_{\text{Cl-Si}}^0(\text{opt}) = 2.140$  Å,  $d_{\text{Si-O}}^0(\text{opt}) = 1.723$  Å,  $C_1 = C_2 = C = 0.679$ . Then the corresponding reaction path is analytically represented as follows:

$$10^{-(\Delta d_{\text{Cl-Si}}/0.679)} + 10^{-(\Delta d_{\text{Si-O}}/0.679)} = 1; \chi^2 = 0.0003, \quad R = 0.98 \quad (13)$$

Fig. 1 shows that along the curve of Eq. (13), the crystalline structures **1–4** are arranged with the significantly lesser root mean square deviation ( $\chi^2 = 0.0003$ ) as compared to the best correlation

function (Eq. (12)) found conventionally ( $\chi^2 = 0.0010$  for Eq. (11) and 0.0009 for Eq. (12)). Nevertheless, on the relatively narrow interval of the change in  $d_{\text{Cl-Si}}$  measuring 2.2–2.5 Å ( $d_{\text{Si-O}} = 1.8$ –2.1 Å) a difference between Eqs. (12) and (13) is insignificant (see Fig. 1). This difference becomes pronounced only for the large Si–O and Cl–Si distances. At  $d_{\text{Si-O}} > 2.1$  Å the correlation function of Eq. (12) overestimates the covalent contribution of the Si–O bond as compared with that of Eq. (13) [**1a** ( $d_{\text{Si-O}} = 2.45$  Å);  $N_{\text{Si-O}} = 0.241$  (Eq. (12)), 0.085 (Eq. (13))]. In contrast, at  $d_{\text{Cl-Si}} > 2.5$  Å it underestimates the ionic component of the Cl–Si bond [**3c** ( $d_{\text{Cl-Si}} = 2.624$  Å);  $N_{\text{Cl-Si}} = 0.375$  (Eq. (12)), 0.194 (Eq. (13))].

The optimal values  $d_{\text{Si-O}}^0(\text{opt}) = 1.723$  Å and  $d_{\text{Cl-Si}}^0(\text{opt}) = 2.140$  Å for the function of Eq. (13) turn out to be  $\sim 0.08$  Å greater than the corresponding experimental values ( $d_{\text{Si-O}}^0(\text{exp}) = 1.639$  Å and  $d_{\text{Cl-Si}}^0(\text{exp}) = 2.065$  Å) which were used in the derivation of Eqs. (11) and (12).<sup>3</sup> How much do the  $d_{\text{Cl-Si}}^0(\text{opt})$  and  $d_{\text{Si-O}}^0(\text{opt})$  values conform with the values of the Cl–Si and Si–O bonds being characteristic of the true reactant (the nonchelate form **A**) and product (the cation **C**) of the studied reaction? It was found that the  $d_{\text{Cl-Si}}$  values for the nonchelate form **A** and the  $d_{\text{Si-O}}$  for cations **C** of compounds **1a–b**, **2a**, and **3a–b**, calculated both with the DFT and MP2 methods, also exceed the corresponding experimental  $d_{\text{Cl-Si}}^0(\text{exp})$  and  $d_{\text{Si-O}}^0(\text{exp})$  values and they are considerably closer to the fitted  $d_{\text{Cl-Si}}^0(\text{opt})$  and  $d_{\text{Si-O}}^0(\text{opt})$  values. For example, for **1b**  $d_{\text{Cl-Si}} = 2.096$  Å in **A** and  $d_{\text{Si-O}} = 1.778$  Å in **C**, according to MP2/6-31G(d) results and, respectively, 2.121 and 1.774 Å, according to the B3LYP/6-31G(d) data.

Thus, the doubts [24,25] about the possibility of describing the reaction coordinate (Eq. (1)) with a classic function of Eq. (5) using the set of crystalline points **1–4** are not supported by the results of our investigation.<sup>4</sup> Actually such a hyperbolic like function (Eq. (13)) describes well the geometrical reconstruction of the ClSi<sub>3</sub>O coordination center of complexes **1–4** during the process of Eq. (1) and includes the reasonable values for  $d_{\text{Cl-Si}}^0$  and  $d_{\text{Si-O}}^0$ . On this basis Eq. (13) can be considered as a reliable analytic representation of the correlation between X-ray values of  $d_{\text{Cl-Si}}$  and  $d_{\text{Si-O}}$  in a series **1–4** and be used for the analysis of quantum-chemical structural information.

### 3.2. Position of the MP2 and DFT optimized gas phase and solution values $d_{\text{Cl-Si}}$ and $d_{\text{Si-O}}$ of compounds **1a–b**, **2a**, and **3a–b** with respect to the crystal structure correlation function (Eq. (13)) of the chelates **1–4**

A series of structures **1a–b**, **2a**, and **3a–b** calculated in the isolated state and in solution with different solvation models (see Tables 2 and 3) may be divided into two groups according to the

<sup>3</sup> A discrepancy between the  $d_{\text{OH}}^0(\text{exp})$  and  $d_{\text{OH}}^0(\text{opt})$  values has been observed also in the MSC modeling of the proton transfer reaction paths with a series of H-complexes having the fragment OH...O [9, 10].

<sup>4</sup> Newly obtained (Eqs. (11) and (12)) are distinct from those found previously [24]. This is due to the fact that we used the improved X-ray results for complex **1a** [38] and invoked new crystalline structures of **1d**, **1h**, **2c**, **2e**, and **4**.

**Table 3**  
MP2 and DFT selected solution bond distances ( $d$  [Å]) and root mean square deviations  $\chi^2$  from the hyperbole of Eq. (13) for species **1a–b**, **2a**, and **3a–b**.

| Model  | Method              | <b>1a</b>         |                    | <b>1b</b>         |                    | <b>2a</b>         |                    | <b>3a</b>         |                    | <b>3b</b>         |                    | $\chi^2$ |
|--|---------------------|-------------------|--------------------|-------------------|--------------------|-------------------|--------------------|-------------------|--------------------|-------------------|--------------------|----------|
|  |                     | $d_{\text{Si-O}}$ | $d_{\text{Si-Cl}}$ | $d_{\text{Si-O}}$ | $d_{\text{Si-Cl}}$ | $d_{\text{Si-O}}$ | $d_{\text{Si-Cl}}$ | $d_{\text{Si-O}}$ | $d_{\text{Si-Cl}}$ | $d_{\text{Si-O}}$ | $d_{\text{Si-Cl}}$ |          |
| <i>CHCl<sub>3</sub> solution (<math>\epsilon = 4.9</math>)</i> |                     |                   |                    |                   |                    |                   |                    |                   |                    |                   |                    |          |
| SCRF   | BP86/6-31G(d)       | 2.364             | 2.204              | 2.094             | 2.275              | 2.198             | 2.218              | 2.083             | 2.261              | 1.972             | 2.323              | 0.0006   |
|  | B3LYP/6-31G(d)      | 2.505             | 2.175              | 2.096             | 2.268              | 2.196             | 2.215              | 2.067             | 2.261              | 1.926             | 2.356              | 0.0003   |
|  | B3PW91/6-31G(d)     | 2.388             | 2.177              | 2.084             | 2.249              | 2.172             | 2.202              | 2.050             | 2.247              | 1.933             | 2.319              | 0.0001   |
| PCM/UAO  | B3PW91/6-311G(2d,p) | 2.380             | 2.183              | 2.042             | 2.279              | 2.170             | 2.209              | 2.034             | 2.261              | 1.918             | 2.333              | 0.0002   |
|  | MP2/6-31G(d)        | 2.309             | 2.187              | 2.064             | 2.255              | 2.156             | 2.204              | 2.025             | 2.263              | 1.922             | 2.338              | 0.0001   |
|  | BP86/6-31G(d)       | 2.290             | 2.241              | 2.065             | 2.316              | 2.139             | 2.262              | 2.024             | 2.327              | 1.932             | 2.403              | 0.0032   |
|  | B3LYP/6-31G(d)      | 2.337             | 2.228              | 2.046             | 2.324              | 2.143             | 2.256              | 1.997             | 2.341              | 1.890             | 2.456              | 0.0030   |
|  | B3LYP/6-311G(d)     | 2.488             | 2.209              | 2.044             | 2.358              | 2.172             | 2.265              | 2.001             | 2.372              | 1.857             | 2.592              | 0.0091   |
|  | B3PW91/6-31G(d)     | 2.248             | 2.229              | 2.035             | 2.302              | 2.114             | 2.246              | 1.987             | 2.319              | 1.899             | 2.400              | 0.0008   |
| SM   | B3PW91/6-311G(2d,p) | 2.273             | 2.228              | 2.017             | 2.319              | 2.119             | 2.249              | 1.974             | 2.336              | 1.866             | 2.445              | 0.0010   |
|  | MP2/6-31G(d)        | 2.266             | 2.208              | 2.086             | 2.253              | 2.132             | 2.223              | 1.995             | 2.292              | 1.921             | 2.347              | 0.0001   |
|  | B3LYP/6-31G(d)      | 2.274             | 2.252              | 2.074             | 2.311              | 2.116             | 2.277              | 1.970             | 2.367              | 1.892             | 2.455              | 0.0038   |
|  | B3PW91/6-31G(d)     | 2.216             | 2.242              | 2.063             | 2.287              | 2.103             | 2.255              | 1.968             | 2.335              | 1.900             | 2.399              | 0.0009   |
| <i>DMSO solution (<math>\epsilon = 46.7</math>)</i>            |                     |                   |                    |                   |                    |                   |                    |                   |                    |                   |                    |          |
| SCRF   | BP86/6-31G(d)       | 2.294             | 2.222              | 2.045             | 2.309              | 2.173             | 2.228              | 2.066             | 2.268              | 1.955             | 2.339              | 0.0009   |
|  | B3LYP/6-31G(d)      | 2.426             | 2.190              | 2.044             | 2.301              | 2.205             | 2.212              | 2.046             | 2.271              | 1.898             | 2.396              | 0.0005   |
|  | B3PW91/6-31G(d)     | 2.323             | 2.191              | 2.044             | 2.273              | 2.144             | 2.213              | 2.034             | 2.254              | 1.911             | 2.344              | 0.0001   |
| PCM/UAO  | B3PW91/6-311G(2d,p) | 2.278             | 2.209              | 1.980             | 2.329              | 2.127             | 2.227              | 2.005             | 2.276              | 1.900             | 2.353              | 0.0004   |
|  | MP2/6-31G(d)        | 2.199             | 2.226              | 2.010             | 2.307              | 2.113             | 2.230              | 1.988             | 2.303              | 1.883             | 2.423              | 0.0004   |
|  | BP86/6-31G(d)       | 2.163             | 2.300              | 2.012             | 2.376              | 2.093             | 2.299              | 1.988             | 2.374              | 1.894             | 2.490              | 0.0077   |
|  | B3LYP/6-31G(d)      | 2.171             | 2.293              | 1.974             | 2.410              | 2.089             | 2.296              | 1.944             | 2.414              | 1.830             | 2.662              | 0.0114   |
|  | B3LYP/6-311G(d)     | 2.221             | 2.301              | 1.935             | 2.523              | 2.084             | 2.330              | 1.901             | 2.535              | 1.744             | 3.526              | 0.0868   |
|  | B3PW91/6-31G(d)     | 2.131             | 2.284              | 1.978             | 2.367              | 2.067             | 2.281              | 1.952             | 2.367              | 1.861             | 2.502              | 0.0032   |
| PCM/UAHF   | B3PW91/6-311G(2d,p) | 2.139             | 2.289              | 1.945             | 2.405              | 2.058             | 2.294              | 1.918             | 2.412              | 1.809             | 2.633              | 0.0046   |
|  | MP2/6-31G(d)        | 2.346             | 2.171              | 2.081             | 2.235              | 2.176             | 2.188              | 2.052             | 2.237              | 1.941             | 2.300              | 0.0004   |
|  | B3LYP/6-31G(d)      | 2.403             | 2.204              | 2.068             | 2.294              | 2.168             | 2.236              | 2.024             | 2.306              | 1.915             | 2.393              | 0.0012   |
|  | B3PW91/6-31G(d)     | 2.251             | 2.217              | 2.053             | 2.277              | 2.135             | 2.226              | 2.017             | 2.285              | 1.912             | 2.362              | 0.0002   |
|  | B3PW91/6-311G(2d,p) | 2.302             | 2.212              | 2.032             | 2.296              | 2.135             | 2.233              | 2.000             | 2.303              | 1.879             | 2.403              | 0.0004   |

values of their root mean square deviation,  $\chi^2$ , from the correlation function of Eq. (13) obtained using X-ray data.

To the first group we assigned theoretical points with  $\chi^2$  values less than or equal to 0.0005 (see Fig. 2 and Tables 2 and 3), which are comparable in magnitude with  $\chi^2 \sim 0.0003$  characteristic of the crystalline complexes **1–4**.

Regardless of the basis set size, all DFT computational schemes (B3LYP, BP86, B3PW91, M05-2X) applied give the gas phase structures which deviate insignificantly ( $\chi^2 \leq 0.0005$ ) from the curve of Eq. (13). In the continuum PCM/UAO model, good theoretical points for **1a**, **2a**, and **3a–b** in the low and high polarity solutions were obtained only when the MP2 method was used. The less complicated Onsager model in a conjunction with the DFT methods (B3LYP, B3PW91) also leads to the solvated structures **1a**, **2a**, and **3a–b** belonging to this group. Judging by the  $\chi^2$  values, (O–Si)chelates **1a**, **2a**, and **3a–b**, deformed by hydrogen bonds with  $\text{CHCl}_3$  (effect

of specific solvation; see Chart 2), are grouped along the curve of Eq. (13) at the MP2 level of theory and markedly deviate from this curve at the B3PW91 level (see Fig. 3 and Table 3).

The location of ab initio and DFT calculated points on the curve of Eq. (13) suggests that some levels of theory adequately reproduce the experimentally established inverse correlation character of the interdependence between the axial Si–O and Cl–Si components in the  $\text{ClSiC}_3\text{O}$  coordination center. However, it is clear that this does not yet guarantee a good quality for each of the pair of the interrelated  $d_{\text{Si-O}}$  and  $d_{\text{Cl-Si}}$  values. Indeed, the analysis of data from Tables 2 and 3 shows that the ( $d_{\text{Cl-Si}}$ ,  $d_{\text{Si-O}}$ ) point which corresponds to complex **1a** can considerably move along the curve of Eq. (13) (within 0.12 Å in the  $d_{\text{Si-O}}$  coordinate) depending on the computational methods of the first group ( $\chi^2 \leq 0.0005$ ).

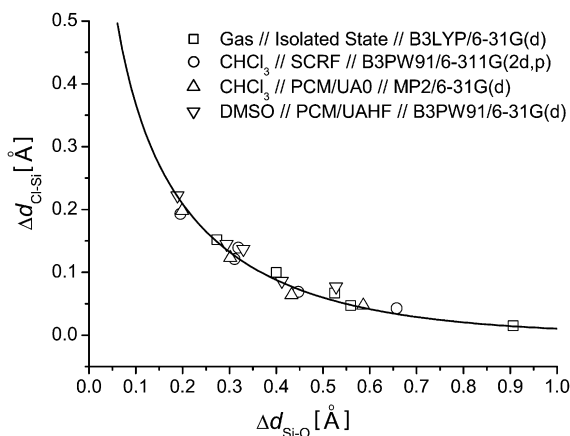


**Fig. 2.** Position of the ab initio and DFT optimized structures **1a**, **2a**, and **3a–b** with the root mean square deviation  $\chi^2 \leq 0.0005$  with respect to the curve of Eq. (13).

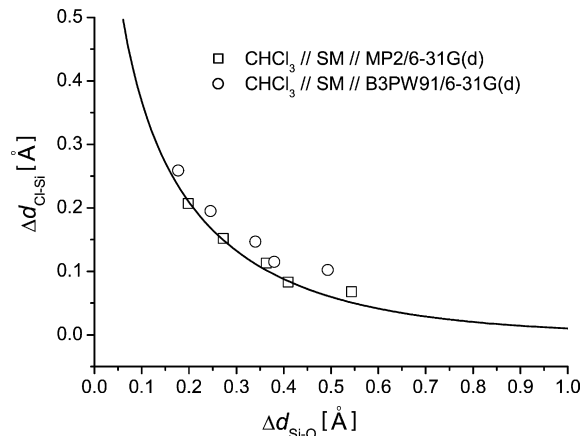


**Fig. 3.** Position of the MP2 and B3PW91 optimized H-complexes of **1a**, **2a**, and **3a–b** with respect to the curve of Eq. (13).



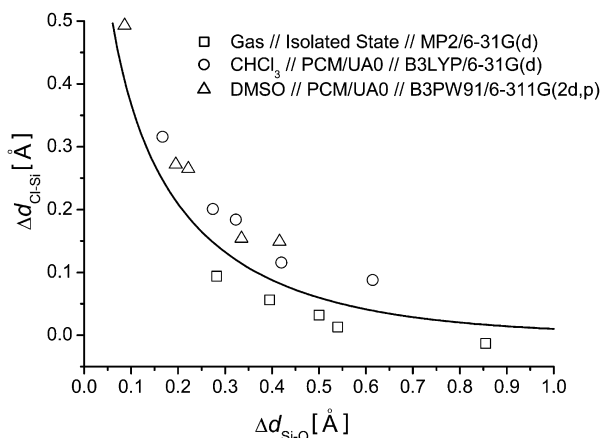


**Fig. 4.** Position of the MP2 and DFT optimized structures **1a–b**, **2a**, and **3a–b** with the root mean square deviation  $\chi^2$  greater than 0.0005 with respect to the curve of Eq. (13).

The second group of structures is characterized by the  $\chi^2$  values greater than 0.0005 (see Fig. 4). Their respective points significantly deviate from the curve of Eq. (13).

The most ‘bad’ lengths of the Si–O and Cl–Si bonds were obtained when combining the solvation PCM/UA0 model with the DFT methods regardless of the value of dielectric constant  $\epsilon$  (see Table 3 and Fig. 4). It seems likely that the PCM/UA0 parameters, i.e. the UFF radii of atomic spheres, are not optimal for predicting the geometry of (O–Si)chelates **1–4** in solution at the PCM/DFT level of theory.<sup>5</sup> The PCM/UAHF model, which uses the HF optimized atomic radii, is considerably more preferable for the DFT methods. The best results are obtained at the PCM/UAHF–B3PW91 level of theory. The geometry parameters of the ClSiC<sub>3</sub>O CC of **1a–b**, **2a**, and **3a–b**, calculated with this computational scheme, are excellently described by the correlation (Eq. (13)) (see Table 3 and Fig. 2). The  $\chi^2$  value is markedly lowered (by a factor  $\sim 10$ , see Table 3) also when PCM/UAHF is combined with the B3LYP functional. However, the PCM/UAHF–B3LYP/6-31G(d) solution points ( $d_{\text{Cl-Si}}$ ,  $d_{\text{Si-O}}$ ) still remain ‘bad’. For the MP2/6-31G(d) method the use of the PCM/UAHF model instead of PCM/UA0 had no effect on the accuracy of the geometry calculation for **1a–b**, **2a**, and **3a–b** in solutions (see Table 3).

A noticeable deviation of the DFT (especially B3LYP) calculated ( $d_{\text{Cl-Si}}$ ,  $d_{\text{Si-O}}$ ) points, which correspond to the structures **1a–b**, **2a**, and **3a–b** solvated specifically in the SM model (B3PW91:  $\chi^2 = 0.0009$ ; B3LYP:  $\chi^2 = 0.0038$ ), from the curve of Eq. (13) (see Fig. 3 and Table 3) may be a consequence of the uncertainties in reproducing the energetics of the formation of weak intermolecular complexes by the density functional theory methods [51].

The MP2 optimized species **1a–b**, **2a**, and **3a–b** in the isolated state fell into the second group of structures. The increase in the basis set size from 6-31G(d) to 6-311++G(d,p) results in the decrease in the  $\chi^2$  value (see Table 2), however, the situation does not become better fundamentally. At the same time this amelioration seems quite possible when using other type basis sets (for example, the Dunning–Huzinaga ones [52]).

The substantial deviation of ab initio and DFT optimized structures from the curve of Eq. (13) may be a warning of the unreliable

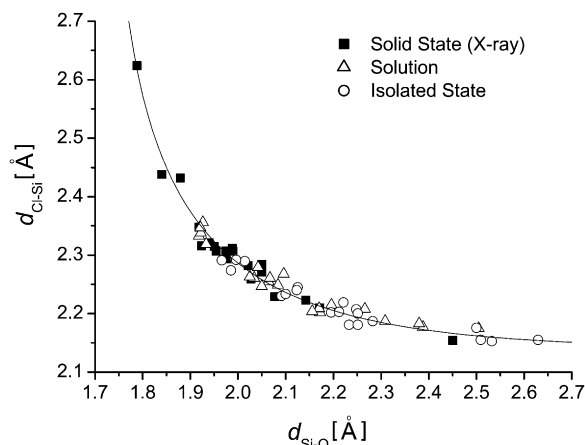


**Fig. 5.** Scatter plot of Cl–Si versus Si–O bond distances for calculated gas-phase, solution and experimental crystal structures of complexes **1–4** ( $\chi^2 \leq 0.0005$ ).

estimation of one or another theoretical axial bond length. For example, judging from Fig. 4, the MP2 method overestimates the Cl–Si or Si–O contact in the isolated state of species **1a–b**, **2a**, and **3a–b**. It is necessary to increase the  $d_{\text{Cl-Si}}$  value by  $\sim 0.03$  Å (leaving the  $d_{\text{Si-O}}$  value unaltered!) or the  $d_{\text{Si-O}}$  value by  $\sim 0.06$  Å (without changing the  $d_{\text{Cl-Si}}$  value) for improving drastically the position of corresponding points ( $d_{\text{Cl-Si}}$ ,  $d_{\text{Si-O}}$ ) with respect to the curve of Eq. (13).

Fig. 5 shows clearly that the major part of ‘good’ theoretical points ( $\chi^2 \leq 0.0005$ ) corresponding to (O–Si)chelates **1a–b**, **2a**, and **3a–b** with the gas phase and solution geometry falls into the region of large internuclear  $d_{\text{SiO}}$  distances ( $> 2.1$  Å), which is poorly filled with crystalline structures **1–4**. Thereby, the use of these structures undoubtedly aids in a more realistic description of the S<sub>N</sub>2 substitution reaction coordinate at Si<sup>IV</sup>.

The use of the values of deviations  $\chi^2$  from the correlation function of Eq. (13), obtained with X-ray data, for the estimation of the reliability of ab initio and DFT calculated gas phase and solution structures **1–4** has led to reasonable rather than discouraging results. For example, unsatisfactory reproduction of the experimental GED values of Hal–Si bond lengths (Hal = F, Cl) with the MP2 method has been mentioned in the literature [53–55]. The observed distinction between the optimal parameters of the PCM model for different calculation methods was reported well [14].

Among the used MP2 and DFT calculation methods, only at the B3PW91 level of theory we succeeded to describe adequately all array of the gas-phase and solution (SCRF, PCM/UAHF approaches)  $d_{\text{Cl-Si}}$  and  $d_{\text{Si-O}}$  values for **1a–b**, **2a**, and **3a–b** with the crystal structure correlation function of Eq. (13). Basing on the criterion ( $\chi^2 \leq 0.0005$ ), one should note also the excellent results of the MP2 method in establishing the geometry of complexes **1–4** in solutions using the PCM and SM approaches. The MP2 and B3PW91 results suggest with confidence that the deformation of the ClSiC<sub>3</sub>O coordination center in the series of **1–4**, caused by the change in its intramolecular environment and medium effects, is really governed by the general regularity of Eq. (13) and corresponds to that expected in the course of the S<sub>N</sub>2 reaction.

#### 4. Conclusions

Using a representative series of the X-ray studied intramolecular complexes **1–4** (*N*-dimethylchlorosilylmethyl derivatives of amides, lactams, carbamides, and hydrazides of carbon acids) possessing an identical ClSiC<sub>3</sub>O coordination center, a mapping of the S<sub>N</sub>2 substitution reaction at Si<sup>IV</sup> has been performed with the structural correlation method. It is possible to obtain a classic

<sup>5</sup> The performance of the PCM model depends on the parameters characterizing a solvent cavity in which a solute is enclosed. Among these are the radii of spheres around atoms as well as the type of molecular surface representing the solute–solvent boundary (solvent excluding, solvent accessible or van der Waals surface) [14,36]. Such parameters, optimized for certain basis sets and quantum mechanical levels of theory, work not so good with other basis sets and theory levels, and the performance of the PCM model with given parameters depends on the molecular properties studied [14].

analytic representation of the reaction coordinate ( $10^{-(\Delta d_{\text{Cl-Si}}/0.679)} + 10^{-(\Delta d_{\text{Si-O}}/0.679)} = 1$ ) using the nonlinear least squares method. The value of the root mean square deviation  $\chi^2$  of the theoretical points ( $d_{\text{Cl-Si}}$ ,  $d_{\text{Si-O}}$ ) from the crystal structure correlation function of Eq. (13) was suggested to use (in the absence of experimental data) as an indicator of the reliability of calculated geometries of related compounds in their isolated state and in solutions. The MP2 and DFT (B3LYP, BP86, B3PW91, M05-2X) gas phase and solution (SCRF, PCM, SM) values of the axial Cl–Si and Si–O bond lengths in complexes **1a–b**, **2a**, and **3a–b** are analyzed in the framework of this criterion. The results obtained suggest that the deformation of the  $\text{ClSiC}_3\text{O}$  coordination center of complexes **1–4**, induced by the change in its intramolecular environment and medium effects, may be well described by one function of Eq. (13). This corroborates the SCM hypothesis of the unified character of the change in the reaction center geometry parameters of related structures under the influence of internal and external factors. Among the used MP2 and DFT methods, only at the B3PW91 level of theory we succeeded to describe adequately all the array of the gas-phase and solution (SCRF, PCM/UAHF approaches)  $d_{\text{Cl-Si}}$  and  $d_{\text{Si-O}}$  values for **1a–b**, **2a**, and **3a–b** with the crystal structure correlation function of Eq. (13). Excellent results for the geometry of the complexes **1–4** in solutions were obtained using the MP2 method with the PCM/UAHF, PCM/UAHF, and SM approaches. Basing on the criterion ( $\chi^2 \leq 0.0005$ ) we established that the combination of the PCM/UAHF model with the DFT methods lead to the unreliable geometries of the complexes **1–4** in polar solutions. The use of the DFT calculation schemes with the polarizable continuum model in the PCM/UAHF version is preferable for obtaining the solution structural parameters of the studied (O–Si)chelates.

## Acknowledgements

The authors are grateful to Prof. I.S. Ignatyev for careful reading of the manuscript and valuable suggestions and to Dr. V.I. Smirnov for assistance with computations using the Gaussian programs. Financial support of our work by the International Association for the Promotion of Cooperation with Scientists from the New Independent States of the Former Soviet Union (INTAS, Grant No. 03-51-4164) and by the Russian Federation President Grant (NS-255.2008.3) is gratefully acknowledged.

## References

- [1] H.-B. Bürgi, J.D. Dunitz, *Acc. Chem. Res.* 16 (1983) 153–161.
- [2] H.-B. Bürgi, J.D. Dunitz, in: H.-B. Bürgi, J.D. Dunitz (Eds.), *Structure Correlation*, Verlag Chemie, Weinheim, 1994.
- [3] H.-B. Bürgi, *Acta Cryst. A54* (1998) 873–885.
- [4] T.R. Ward, H.-B. Bürgi, F. Gilardoni, J. Weber, *J. Am. Chem. Soc.* 119 (1997) 11974–11985.
- [5] V. Ferretti, V. Bertolasi, P. Gilli, G. Gilli, *Phys. Chem. Chem. Phys.* 1 (1999) 2303–2309.
- [6] S. Alvarez, M.J. Lluell, *Chem. Soc. Dalton Trans.* (2000) 3288–3303.
- [7] A.R. Bassindale, M. Borbaruah, S.J. Glunn, D.J. Parker, P.G. Taylor, *J. Chem. Soc. Perkin Trans. 2* (1999) 2099–2109.
- [8] V.F. Sidorkin, V.V. Vladimirov, M.G. Voronkov, V.A. Pestunovich, *J. Mol. Struct. (THEOCHEM)* 228 (1991) 1–9.
- [9] P. Gilli, V. Bertolasi, V. Ferretti, G. Gilli, *J. Am. Chem. Soc.* 116 (1994) 909–915.
- [10] S.J. Grabowski, *J. Mol. Struct.* 552 (2000) 153–157.
- [11] D.J. Hankinson, J. Almlöf, K.R. Leopold, *J. Phys. Chem.* 100 (1996) 6904–6909.
- [12] H.-B. Bürgi, in: A.F. Williams, C. Floriani, A.E. Merbach (Eds.), *Perspectives in Coordination Chemistry*, Verlag Helvetica Chimica Acta, Basel, 1992, pp. 1–30.
- [13] M.A. Dvorak, R.S. Ford, R.D. Suenram, F.J. Lovas, K.R. Leopold, *J. Am. Chem. Soc.* 114 (1992) 108–114.
- [14] J. Tomasi, R. Cammi, B. Mennucci, C. Cappelli, S. Corni, *Phys. Chem. Chem. Phys.* 4 (2002) 5697–5712.
- [15] C. Cappelli, S. Corni, B. Mennucci, R. Cammi, J. Tomasi, *J. Phys. Chem. A* 106 (2002) 12331–12339.
- [16] B. Mennucci, J. Tomasi, R. Cammi, J.R. Cheeseman, M.J. Frisch, F.J. Devlin, S. Gabriel, P.J. Stephen, *J. Phys. Chem. A* 106 (2002) 6102–6113.
- [17] R. Cammi, B. Mennucci, J. Tomasi, *J. Chem. Phys.* 110 (1999) 7627–7638.
- [18] V. Vallet, P. Macac, U. Wahlgren, I. Grenthe, *Theor. Chem. Acc.* 115 (2006) 145–160.
- [19] R. Sayós, J. Hernando, J. Daniel Sierra, M.A. Rodríguez, M. González, *Phys. Chem. Chem. Phys.* 3 (2001) 4701–4711.
- [20] V.F. Sidorkin, E.F. Belogolova, V.A. Pestunovich, *J. Mol. Struct. (THEOCHEM)* 538 (2001) 59–65.
- [21] V.A. Pestunovich, V.F. Sidorkin, M.G. Voronkov, in: B. Marciniec, J. Chojnowski (Eds.), *Progress in Organosilicon Chemistry*, Gordon and Breach Science Publishers, New York, 1995, pp. 69–82.
- [22] M.G. Voronkov, V.A. Pestunovich, Yu.A. Baukov, *Metalloorgan. Khim. (Russ.)* 4 (1991) 1210–1227 (*Organomet. Chem. USSR (Engl. Transl.)* 4 (1991) 593–608).
- [23] D. Kost, I. Kalikhman, in: Z. Rappoport, Y. Apeloig (Eds.), *The Chemistry of Organic Silicon Compounds*, Wiley, Chichester, 1998, pp. 1339–1445.
- [24] A.O. Mozhukhin, M.Yu. Antipin, Yu.T. Struchkov, A.G. Shipov, E.P. Kramarova, Yu.I. Baukov, *Metalloorg. Khim. (Russ.)* 5 (1992) 917–924 (*Organomet. Chem. USSR (Engl. Transl.)* 5 (1992)).
- [25] Yu.E. Ovchinnikov, A.A. Macharashvili, Yu.T. Struchkov, A.G. Shipov, Yu.I. Baukov, *Zh. Strukt. Khim. (Russ.)* 35 (1994) 100–110 (*J. Struct. Chem. USSR (Engl. Transl.)* 35 (1994) 91).
- [26] Ya. Zhao, D.G. Truhlar, *Theor. Chem. Acc.* 120 (2008) 215–241.
- [27] M. Szafraan, M.M. Karelson, A.R. Katritzky, J. Koput, M.C. Zerner, *J. Comput. Chem.* 14 (1993) 371–377.
- [28] M.T. Cancès, B. Mennucci, J. Tomasi, *J. Chem. Phys.* 107 (1997) 3032–3037.
- [29] B. Mennucci, J. Tomasi, *J. Chem. Phys.* 106 (1997) 5151–5158.
- [30] A. Pullman, in: R. Daudel (Ed.), *Quantum Theory of Chemical Reaction*, Reidel, Amsterdam, 1980.
- [31] V.N. Khrustalev, I.A. Portnyagin, I.V. Borisova, N.N. Zemlyansky, Yu.A. Ustynyuk, M.Yu. Antipin, M.S. Nechaev, *Organometallics* 25 (2006) 2501–2504.
- [32] M.W. Wong, K.B. Wiberg, M.J. Frisch, *J. Chem. Phys.* 95 (1991) 8991–8998.
- [33] A.K. Rappé, C.J. Casewit, K.S. Colwell, W.A. Goddard III, W.M. Skiff, *J. Am. Chem. Soc.* 114 (1992) 10024–10035.
- [34] V. Barone, M. Cossi, J. Tomasi, *J. Chem. Phys.* 107 (1997) 3210–3221.
- [35] M.W. Schmidt, K.K. Baldridge, J.A. Boatz, S.T. Elbert, M.S. Gordon, J.J. Jensen, S. Koseki, N. Matsunaga, K.A. Nguyen, S. Su, T.L. Windus, M. Dupuis, J.A. Montgomery, *J. Comput. Chem.* 14 (1993) 1347–1363.
- [36] M.J. Frisch, G.W. Trucks, H.B. Schlegel, G.E. Scuseria, M.A. Robb, J.R. Cheeseman, J.A. Montgomery Jr., T. Vreven, K.N. Kudin, J.C. Burant, J.M. Millam, S.S. Iyengar, J. Tomasi, V. Barone, B. Mennucci, M. Cossi, G. Scalmani, N. Rega, G.A. Petersson, H. Nakatsuji, M. Hada, M. Ehara, K. Toyota, R. Fukuda, J. Hasegawa, M. Ishida, T. Nakajima, Y. Honda, O. Kitao, H. Nakai, M. Klene, X. Li, J.E. Knox, H.P. Hratchian, J.B. Cross, C. Adamo, J. Jaramillo, R. Gomperts, R.E. Stratmann, O. Yazyev, A.J. Austin, R. Cammi, C. Pomelli, J.W. Ochterski, P.Y. Ayala, K. Morokuma, G.A. Voth, P. Salvador, J.J. Dannenberg, V.G. Zakrzewski, S. Dapprich, A.D. Daniels, M.C. Strain, O. Farkas, D.K. Malick, A.D. Rabuck, K. Raghavachari, J.B. Foresman, J.V. Ortiz, Q. Cui, A.G. Baboul, S. Clifford, J. Cioslowski, B.B. Stefanov, G. Liu, A. Liashenko, P. Piskorz, I. Komaromi, R.L. Martin, D.J. Fox, T. Keith, M.A. Al-Laham, C.Y. Peng, A. Nanayakkara, M. Challacombe, P.M.W. Gill, B. Johnson, W. Chen, M.W. Wong, C. Gonzalez, J.A. Pople, *Gaussian 03*, Revision B.03, Gaussian, Inc., Pittsburgh PA, 2003.
- [37] P.R. Bevington, D.K. Robinson, *Data Reduction and Error Analysis for the Physical Sciences*, McGrawHill, New York, 1992.
- [38] O.B. Artamkina, E.P. Kramarova, A.G. Shipov, Yu.I. Baukov, A.A. Macharashvili, Yu.E. Ovchinnikov, Yu.T. Struchkov, *Zh. Obshch. Khim. (Russ.)* 64 (1994) 263–272 (*Russ. J. Gen. Chem. (Engl. Transl.)* (1994) 64).
- [39] A.R. Bassindale, D.J. Parker, P.G. Taylor, N. Auner, B. Herrschaft, *J. Organomet. Chem.* 667 (2003) 66–72.
- [40] S.A. Pogozhikh, Yu.E. Ovchinnikov, E.P. Kramarova, V.V. Negrebetskii, A.G. Shipov, A.I. Albanov, M.G. Voronkov, V.A. Pestunovich, Yu.I. Baukov, *Zh. Obshch. Khim. (Russ.)* 74 (2004) 1617–1624 (*Russ. J. Gen. Chem. (Engl. Transl.)* 74 (2004) 1501).
- [41] A.O. Mozhukhin, M.Yu. Antipin, Yu.T. Struchkov, A.G. Shipov, E.P. Kramarova, Yu.I. Baukov, *Metalloorg. Khim. (Russ.)* 5 (1992) 906–916 (*Organomet. Chem. USSR (Engl. Transl.)* 5 (1992) 439).
- [42] A.A. Macharashvili, V.E. Shklover, Yu.T. Struchkov, M.G. Voronkov, B.A. Gostevskii, I.D. Kalikhman, O.B. Bannikova, V.A. Pestunovich, *Metalloorg. Khim. (Russ.)* 1 (1988) 1131–1134 (*Organomet. Chem. USSR (Engl. Transl.)* 1 (1988)).
- [43] Yu.I. Baukov, Yu.E. Ovchinnikov, A.G. Shipov, E.P. Kramarova, V.V. Negrebetskii, Yu.T. Struchkov, *J. Organomet. Chem.* 536–537 (1997) 399–403.
- [44] A.R. Bassindale, S.J. Glynn, P.G. Taylor, N. Auner, B. Herrschaft, *J. Organomet. Chem.* 619 (2001) 132–140.
- [45] S. Wolfe, D.J. Mitchell, H.B. Schlegel, *J. Am. Chem. Soc.* 103 (1981) 7692–7694.
- [46] N.L. Arthur, J.A. McDonnell, *J. Chem. Phys.* 56 (1972) 3100–3110.
- [47] S.W. Mayer, *J. Phys. Chem.* 73 (1969) 3941–3946.
- [48] L. Pauling, *J. Am. Chem. Soc.* 69 (1947) 542–553.
- [49] J.D. Dunitz, *X-Ray Analysis and the Structure of Organic Molecules*, Cornell University Press, Ithaca, 1979.
- [50] H.S. Johnston, C. Parr, *J. Am. Chem. Soc.* 85 (1963) 2544–2551.
- [51] P.R. Schreine, *Angew. Chem. Int. Ed.* 46 (2007) 4217–4219.
- [52] T.H. Dunning Jr., P.J. Hay, in: H.F. Schaefer III (Ed.), *Modern Theoretical Chemistry*, Plenum, New York, 1976, pp. 1–28.
- [53] M. Dakkouri, M. Grosser, *J. Mol. Struct.* 559 (2001) 7–24.
- [54] S.L. Hinchley, H.E. Robertson, D.W.H. Rankin, W.-W. du Mont, *J. Chem. Soc. Dalton Trans.* (2002) 3787–3794.
- [55] U. Losehand, N.W. Mitzel, D.W.H. Rankin, *J. Chem. Soc. Dalton Trans.* (1999) 4291–4297.